Arch. Mech., 36, 3, pp. 365–378, Warszawa 1984

# Laminar separation instability on a convex surface in relation to periodic vortex shedding (*)

Y. C. SUN (GÖTTINGEN)

LAMINAR separation instability in a two-dimensional incompressible flow over a convex surface at low Reynolds numbers is investigated by the aid of a new stability equation derived in the knowledge of the asymptotic triple-deck model of flow. The results of the stability analysis show the existence of a critical Reynolds number of about 60 and of a distinct wavelength-frequency relationship for the maximum amplification of instability. The notable aspect of this relationship consits in the apparent lack of preference for any definite combination of wave-length and frequency for the maximum amplification. This should open the way for the influence of the external excitation, such as the near-wake instability, on the separation instability and consequently on the vortex shedding as well.

Analiza stateczności wskazuje na istnienie krytycznej liczby Reynoldsa wynoszącej około 60 oraz wyraźnej zależności między częstością a długością fali dla maksymalnego wzmocnienia niestateczności. Ważnym aspektem tego związku jest brak jakiejkolwiek preferencji dla konkretnej kombinacji tych wielkości. Fakt ten powinien otworzyć drogę dla wpływu wzbudzenia zewnętrznego, jak np. niestateczności w sąsiedztwie śladu, na niestateczność oderwania oraz także na proces spływu zawirowań.

Анализ устойчивости указывает на существование критического числа Рейнольдса, равняющегося примерно 60, а также отчетливой зависимости между частотой и длиной волны для максимального усиления неустойчивости. Важным аспектом этой зависимости является отсутствие какого-нибудь предпочтения для конкретной комбинации этих величин. Этот факт должен открыть путь для влияния внешнего возбуждения, как например неустойчивости в соседстве следа, на неустойчивость отрыва, а также на процесс стока вихрей.

## 1. Introduction

FLOWS about bluff bodies with convex surfaces are generally characterized by separation and by a strong wake formation. In a wide range of free-stream speeds, the separation on bluff bodies takes the form of periodic vortex shedding.

One of the most conspicuous examples of such flows is represented by the flow about a circular cylinder (Fig. 1). In such a flow, at very low Reynolds numbers (Re), the flow is attached (Fig. 1a). At higher Re, separation appears and the separation zone in the form of two standing vortices moves towards the front with increasing Re. At some critical Re ($\approx 50$), wake fluctuation attributable to the incipient periodic vortex shedding begins to take place, thus lending periodicity to the wake and the flow as a whole (Fig. 1b). As the Re further increases, the relatively steady separation zone in the form of standing vortices breaks down and downstream the well-known Kármán vortex street begins to make its

(*) Paper given at XVI Symposium on Advanced Problems and Methods in Fluid Mechanics, Spała, 4–10 September, 1983.

http://rcin.org.pl

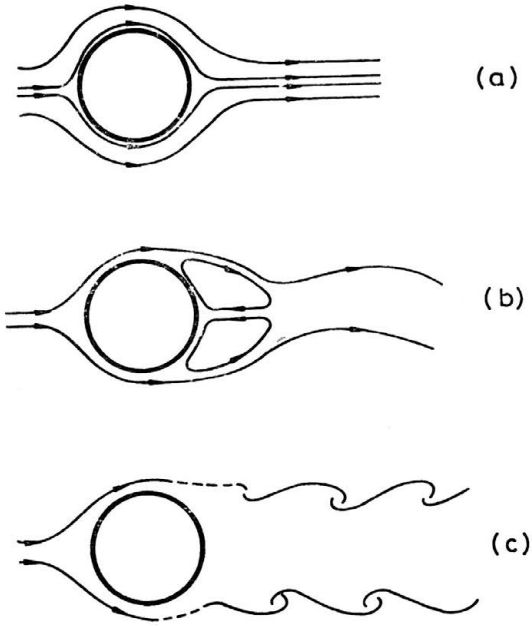


FIG. 1. Forms of flow over a circular cylinder.

appearance (Fig. 1c). At still higher Re (Re > 200/300 in the case of a circular cylinder), the separation points themselves start to fluctuate backwards and forwards noticeably, rendering the separation periodic in space and time.

The problem of periodic vortex shedding is important from the practical point of view, for example for flows over slender bodies like missiles at high angles of attack. The origination and the mechanism of periodic vortex shedding are, however, not quite clear yet. Owing to the periodicity of the phenomenon, it is natural to postulate a close relationship of the periodic vortex shedding to some form of flow instability. According to a number of investigations ([1]–[4] among others), the periodic vortex shedding seems to be closely related to the instability of wake structure. Moreover, it is known from earlier experiments (e.g. [5]–[7]) that a splitter plate of sufficient length attached to the rear stagnation point of a circular cylinder can destroy the periodic vortex shedding and suppress the vortex-street formation. This suggests the strong influence of the wake instability on the periodic vortex shedding. In spite of the apparently eminent role played by the wake instability in the origination of periodic vortex shedding, the flow instability at the separation point(s) should take its share of generating the periodic vortex shedding as well. Some flow mechanism must be existent at the separation point(s) which enables the wake instability to exert its influence.

The present work is aimed at giving a renewed study of the flow instability at the separation point on a convex surface with special emphasis on its possible effect on vortex shedding, in the hope of gaining some insight into the mechanism of periodic vortex shedding. The previous investigations of separation instability ([8]–[10]) among others) have the common features of employing the boundary-layer approximation for the basic

http://rcin.org.pl

flow and of concentrating on the determination of the critical Re which marks the beginning of instability. The present investigation sets out for a different direction in two ways: firstly, the boundary-layer approximation that is known to be not valid in the immediate region of separation (e.g. Goldstein singularity, etc.) is not employed for the basic flow, and secondly, concentration is placed upon the determination of wavelength-frequency combinations giving the maximum amplification of disturbances or the maximum instability. It is believed that the maximum amplification really matters in the generation of periodic vortex shedding. The investigation is confined to laminar on-coming flows of Re under 300, which correspond to the stage of flow prior to the onset of fluctuation of the separation point in the case of a circular cylinder. The flow behaviour at this initial stage of periodic vortex shedding should give some clue to the development of vortex shedding at later stages as well.

## 2. Stability analysis

### 2.1. Flow equations for the separation region

The general equations of two-dimensional incompressible laminar flow over a convex surface consist of (cf e.g. [11]): the $x$-momentum equation

$$(2.1)\qquad (1+\tilde{y})\frac{\partial u}{\partial t}+u\frac{\partial u}{\partial x}+(1+\tilde{y})v\frac{\partial u}{\partial y}+\frac{uv}{r}$$
$$=-\frac{\partial p}{\partial x}+\frac{1}{\mathrm{Re}_L}\left[\frac{1}{1+\tilde{y}}\frac{\partial^2 u}{\partial x^2}+(1+\tilde{y})\frac{\partial^2 u}{\partial y^2}+\frac{1}{r}\frac{\partial u}{\partial y}\right.$$
$$\left.-\frac{1}{r^2(1+\tilde{y})}u+\frac{2}{r(1+\tilde{y})}\frac{\partial v}{\partial x}+\frac{y}{r^2(1+\tilde{y})^2}\frac{dr}{dx}\frac{\partial u}{\partial x}-\frac{1}{r^2(1+\tilde{y})^2}\frac{dr}{dx}v\right],$$

the $y$-momentum equation

$$(2.2)\qquad \frac{\partial v}{\partial t}+\frac{1}{1+\tilde{y}}u\frac{\partial u}{\partial x}+v\frac{\partial v}{\partial y}-\frac{1}{r(1+y)}u^2$$
$$=-\frac{\partial p}{\partial y}+\frac{1}{\mathrm{Re}_L}\left[\frac{1}{(1+\tilde{y})^2}\frac{\partial^2 v}{\partial x^2}+\frac{\partial^2 v}{\partial y^2}+\frac{1}{r(1+\tilde{y})}\frac{\partial v}{\partial y}-\frac{1}{r^2(1+\tilde{y})^2}v\right.$$
$$\left.-\frac{2}{r(1+\tilde{y})^2}\frac{\partial u}{\partial x}+\frac{y}{r^2(1+\tilde{y})^3}\frac{dr}{dx}\frac{\partial v}{\partial x}+\frac{1}{r^2(1+\tilde{y})^3}\frac{dr}{dx}u\right],$$

and the continuity equation

$$(2.3)\qquad \frac{\partial u}{\partial x}+\frac{\partial}{\partial y}[(1+\tilde{y})v]=0,$$

all written out in full. Here $x$, $y$, $t$, $u$, $v$, $r$, $\tilde{y}$, $p$ represent dimensionless variables where:

$$(2.4)\qquad \begin{aligned} &x=\frac{X}{L}, \quad y=\frac{Y}{L}, \quad t=\frac{U_\infty T}{L}, \quad u=\frac{U}{U_\infty},\\ &v=\frac{V}{U_\infty}, \quad r(x)=\frac{R(X)}{L}, \quad \tilde{y}=\frac{y}{r}, \quad p=\frac{P}{\varrho_\infty U_\infty^2}. \end{aligned}$$

http://rcin.org.pl

$X$, $Y$ are the curvilinear coordinates employed with $X$ parallel and $Y$ perpendicular to the wall that is denoted by $R(X)$. $U$, $V$ denote the velocity components in the $X$-and $Y$-directions, respectively, $U_\infty$ being the free-stream speed, $T$ the time variable, $P$ the pressure, $\varrho_\infty$ the density (constant here), and $L$ some characteristic length of the problem. $\mathrm{Re}_L = \dfrac{U_\infty L}{\nu}$ stands for the Reynolds number formed with $L$, $\nu$ being the kinematic viscosity. The quantity $dr/dx$ appearing in several terms of Eqs. (2.1) and (2.2) denotes the measure of the variation of wall radius along the wall and is exactly null when the wall represents a circular arc.

It is to be noted that for the present analysis only a very narrow and relatively shallow region in the immediate vicinity of the separation point is taken into consideration. On this account, $\tilde{y}$ and $dr/dx$ are taken to be small quantities with $\tilde{y} \ll 1$ and $dr/dx \ll 1$. This implies that the relevant flow depth considered is much smaller than the wall radius while the wall in the separation region can be very closely approximated by a circular arc.

Introducing now the stream function $\psi$ such that

$$u = \frac{\partial \psi}{\partial y}, \quad v = -\frac{1}{1+\tilde{y}}\frac{\partial \psi}{\partial x}, \tag{2.5}$$

replacing $L$ by $D(D = 2R_s$, $R_s$ being the wall radius at the separation point $x_{\mathrm{sep}})$ and eliminating the pressure terms in Eqs. (2.1) and (2.2), one arrives at the single equation for $\psi$:

$$(1+\tilde{y})\frac{\partial \Delta\psi}{\partial t} + \frac{\partial \psi}{\partial y}\frac{\partial \Delta\psi}{\partial x} - \frac{\partial \psi}{\partial x}\frac{\partial \Delta\psi}{\partial y} = \frac{1}{\mathrm{Re}_D}(1+\tilde{y})\Delta\Delta\psi \tag{2.6}$$

with

$$\Delta \equiv \frac{1}{(1+\tilde{y})^2}\frac{\partial^2}{\partial x^2} + \frac{\partial^2}{\partial y^2} + \frac{1}{r(1+\tilde{y})}\frac{\partial}{\partial y}.$$

In Eq. (2.6) the linear terms of $\tilde{y}$ with an open order of magnitude are retained in order to include the main curvature effect of the flow.

Approximating $\psi$ by $\psi = \varphi_0 + \varphi$ with $\varphi \ll \varphi_0$, where $\varphi_0$ represents the basic flow satisfying the flow equation in the form of Eq. (2.6) while $\varphi$ signifies some perturbation to the basic flow, one obtains to the first-order linear approximation

$$(1+\tilde{y})\frac{\partial \Delta\varphi}{\partial t} + \frac{\partial \varphi_0}{\partial y}\frac{\partial \Delta\varphi}{\partial x} + \frac{\partial \varphi}{\partial y}\frac{\partial \Delta\varphi_0}{\partial x} - \frac{\partial \varphi_0}{\partial x}\frac{\partial \Delta\varphi}{\partial y} - \frac{\partial \varphi}{\partial x}\frac{\partial \Delta\varphi_0}{\partial y} = \frac{1}{\mathrm{Re}_D}(1+\tilde{y})\Delta\Delta\varphi. \tag{2.7}$$

If now the conventional boundary-layer approximation is adopted for the basic flow, the terms in Eq. (2.7) containing $\dfrac{\partial \Delta\varphi_0}{\partial x}$ and $\dfrac{\partial \varphi_0}{\partial x}$ may be omitted from the beginning. However, in view of the flow structure in the region of separation, the boundary-layer approximation is not employed in the assessment of the basic flow characterized by $\varphi_0$.

http://rcin.org.pl

### 2.2. Equations for stability analysis

The flow at the separation point on a convex surface is known to be fundamentally unstable not only because the velocity profile there necessarily contains a point of inflection owing to the onset of flow reversal but also because the flow over a convex surface is generally unstable against disturbances in the form of Tollmien–Schlichting waves. As previously, the perturbation $\varphi$ to the basic flow is now postulated to be a Tollmien–Schlichting wave. Thus

$$\varphi(x, y, t) = \bar{\varphi}(y) e^{i(\bar{\alpha}x - \bar{\beta}t)}, \tag{2.8}$$

where $\bar{\alpha}$ denotes the dimensionless wave-number with $\bar{\alpha} = \dfrac{2\pi D}{\lambda}$; $\bar{\beta}$ the dimensionless frequency $\bar{\beta} = \beta \dfrac{D}{U_\infty} = \dfrac{2\pi f D}{U_\infty}$, $\lambda$ being the wave length, $f$ the frequency, $\beta$ the cyclic frequency.

The derivation of the appropriate perturbation equations for $\varphi$ from Eq. (2.7) for the stability analysis necessitates a correct assessment of the orders of magnitude of the various terms involving $\varphi_0$. Barring now a tedious, if at all practicable, numerical solution of the full equation for $\varphi_0$ in the form of Eq. (2.6) for $t \to \infty$, some recourse must be made to a rational analytical model which should at least provide the correct orders of magnitude of the $\varphi_0$-terms. For this purpose, the well-known asymptotic triple-deck analytical model for the steady laminar separation flow ([12]–[15]) is utilized (Fig. 2). Strictly speaking,

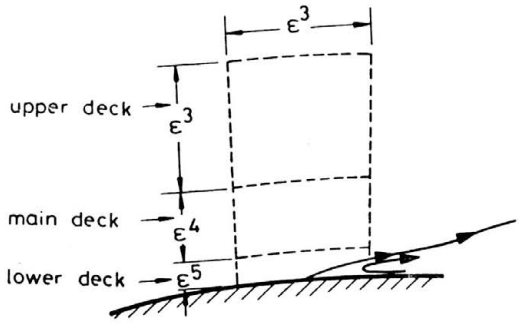


FIG. 2. Triple-deck schematic model.

the basic flow is not entirely steady. But, on the basis of experimental observations, the flow ahead of the separation point(s) is steady or approximately steady prior to the onset of spatial fluctutation of the separation point(s). If the stability analysis now is confined to the separation section $x = x_{sep}$ only, as is the case at present, the application of an analytical model of steady flow in the immediate neighbourhood of separation is justifiable.

The fundamental parameter of the asymptotic triple-deck model is $\varepsilon$ ($\varepsilon = \mathrm{Re}^{-1/8}$). By employment of the Kirchhoff's free-streamline concept for flow detachment, the laminar separation zone is characterized by a longitudinal interaction length $x = O(\varepsilon^3)$, while the transverse interaction zones of the three decks (the lower deck, the main deck and the upper deck) have different depths (Fig. 2). In the lower deck (LD) with $y_{LD} = O(\varepsilon^5)$,

http://rcin.org.pl

a viscous flow of the boundary-layer type is involved. The main deck (MD) with $y_{\mathrm{MD}} = O(\varepsilon^4)$ contains inviscid rotational flow, while potential flow prevails in the upper deck (UD) with $y_{\mathrm{UD}} = O(\varepsilon^3)$.

The available results of the matched asymptotic analysis of the triple-deck model are used to estimate the orders of magnitude of the different terms involving $\varphi_0$ in Eq. (2.7). The velocities in the various decks are known to be:

$$
\begin{aligned}
&u_{0\,\mathrm{LD}} = O(\varepsilon)+\ldots, && v_{0\,\mathrm{LD}} = O(\varepsilon^3)+\ldots,\\
&u_{0\,\mathrm{MD}} = u_m(y)+O(\varepsilon)+\ldots, && v_{0\,\mathrm{MD}} = O(\varepsilon^2)+\ldots,\\
&u_{0\,\mathrm{UD}} = 1+O(\varepsilon^2)+\ldots, && v_{0\,\mathrm{UD}} = O(\varepsilon^2)+\ldots.
\end{aligned}
\tag{2.9}
$$

The orders of magnitude of, for example, $\dfrac{\partial^2 u_0}{\partial y^2}$, $\dfrac{\partial^2 v_0}{\partial x^2}$, $\dfrac{\partial^2 v_0}{\partial y^2}$ of the basic flow for the different decks are:

$$
\begin{aligned}
&\mathrm{LD}\,O(\varepsilon^{-9}), \quad \mathrm{MD}\,O(\varepsilon^{-8}), \quad \mathrm{UD}\,O(\varepsilon^{-4});\\
&\mathrm{LD}\,O(\varepsilon^{-3}), \quad \mathrm{MD}\,O(\varepsilon^{-4}), \quad \mathrm{UD}\,O(\varepsilon^{-4});\\
&\mathrm{LD}\,O(\varepsilon^{-7}), \quad \mathrm{MD}\,O(\varepsilon^{-6}), \quad \mathrm{UD}\,O(\varepsilon^{-4}), \quad \text{respectively.}
\end{aligned}
$$

The disturbance in the separation section $x = x_{\mathrm{sep}}$ represented by Eq. (2.8) in the form of a Tollmien–Schlichting wave possesses the amplitude $\bar{\varphi}(y)$. The orders of magnitude of $\bar{\varphi}$ and its derivatives in the different decks are rated in compliance with the triple-deck analysis. For convenience, they are taken as $\varepsilon^2$ times the corresponding terms for $\varphi_0$. The factor $\varepsilon^2$ here is actually immaterial; a different small factor will also serve the purpose. The orders of magnitude of $\bar{\alpha}$ and $\bar{\beta}$ are so chosen that the dependence of $\bar{\varphi}$ on $\bar{\alpha}$ and $\bar{\beta}$ is assured.

With the basic flow embodying $\varphi_0$ now delineated by the triple-deck model, perturbation equations of the amplitude $\bar{\varphi}$ are derived for the three decks of flow by taking the leading terms of the resultant equations out of Eqs. (2.7) and (2.8):

$$
\begin{aligned}
&(\mathrm{LD}) && \bar{\varphi}''''-\mathrm{Re}_D[v_0\bar{\varphi}'''+i(\bar{\alpha}u_0-\bar{\beta})\bar{\varphi}''-v_{0\,yy}\bar{\varphi}'-i\bar{\alpha}u_{0\,yy}\bar{\varphi}] = 0,\\
&(\mathrm{MD}) && v_0\bar{\varphi}'''+i(\bar{\alpha}u_0-\bar{\beta})\bar{\varphi}''-v_{0\,yy}\bar{\varphi}'-i\bar{\alpha}u_{0\,yy}\bar{\varphi} = 0,\\
&(\mathrm{UD}) && v_0\bar{\varphi}'''+i(\bar{\alpha}u_0-\bar{\beta})\bar{\varphi}''-(v_{0\,xx}+v_{0\,yy})\bar{\varphi}' = 0.
\end{aligned}
\tag{2.10}
$$

Here $u_0$ and $v_0$ refer to the variables of the basic flow, whereas terms with subscripts denote the derivatives involved with respect to the subscripts.

Equation (2.10) can be employed for a multi-scale matched asymptotic analysis which is, in general, much involved and complicated. A much simpler way that yields essentially the same results has been found to use a single equation for $\bar{\varphi}$ in the stability analysis:

$$
\bar{\varphi}'''-\mathrm{Re}_D[v_0\bar{\varphi}'''+i(\bar{\alpha}u_0-\bar{\beta})\bar{\varphi}''-(v_{0\,xx}+v_{0\,yy})\bar{\varphi}'-i\bar{\alpha}u_{0\,yy}\bar{\varphi}] = 0
\tag{2.11}
$$

with the boundary conditions:

$$
\begin{aligned}
&y = 0: \quad \bar{\varphi}' = \bar{\varphi}'' = 0,\\
&y = \bar{y}: \quad \bar{\varphi}' = \bar{\varphi}'' = 0,
\end{aligned}
\tag{2.12}
$$

where $\bar{y}$ denotes some outer boundary of the relevant flow region.

Equation (2.11) is obviously over-complete but by no means incorrect for the main deck and the upper deck. In this manner, except for the later determination of $v_0$ out

http://rcin.org.pl

of $u_0$, the mission of the triple-deck model has been essentially completed in deriving the $\varphi$-equation, correct in orders of magnitude, for the stability analysis. Equation (2.11) contains all the necessary terms and more for the various decks and frees the treatment from the necessity of differential scaling if some plausible unified velocity profile ($u_0$) at $x_{sep}$ with respect to the undistorted geometrical coordinate $y$ can be postulated. This requirement can be fulfilled in that at $x_{sep}$ $u_0$ may be plausibly approximated as

$$u_0 = \hat{y}^2(b-8\hat{y}+3\hat{y}^2), \quad 0 \leqslant \hat{y} \leqslant 1 \tag{2.13}$$

which is known as the Pohlausen polynomial, or as

$$u_0 = 1-\operatorname{sech}^2(n\hat{y}) \quad (n \text{ variable}). \tag{2.14}$$

It is to be noted that the scale of $\hat{y}$ in Eqs. (2.13) and (2.14) remains open yet and can be fixed by a uniform coordinate transformation for the unified Eq. (2.11).

In order to avoid dealing with very small numerical quantities throughout the computation, some transformation or stretching of the coordinate $y$ at $x_{sep}$ is desirable. For convenience, the following uniform transformation and substitutions are introduced for the whole region between $y = 0$ and $y = \bar{y}$ (cf. Eq. (2.12)):

$$\begin{gathered} \hat{y} = \frac{y}{\delta}, \qquad \hat{\varphi} = \frac{\bar{\varphi}}{\delta}, \qquad \hat{\varphi}'(\hat{y}) = \bar{\varphi}'(y), \\ \hat{\varphi}'' = \delta\bar{\varphi}'', \quad \hat{\varphi}''' = \delta^2\bar{\varphi}''', \quad \hat{\varphi}'''' = \delta^3\bar{\varphi}'''', \\ \hat{u}_0 = u_0, \qquad \hat{v}_0 = \frac{\delta}{\varepsilon^3}\bar{v}_0, \end{gathered} \tag{2.15}$$

$\delta$ actually may be arbitrary. For practical purpose $\delta$ is taken as $\varepsilon^4$ and corresponds to the normal boundary-layer thickness.

Such a procedure is allowable since Eq. (2.11) now becomes a unified equation for the whole relevant region at $x_{sep}$ with a uniformly valid velocity profile given by Eq. (2.13) or Eq. (2.14). By Eq. (2.15), with $\delta = \varepsilon^4$, Eq. (2.11) is transformed into

$$\hat{\varphi}'''' - [\varepsilon^{-3}\hat{v}_0\hat{\varphi}''' + i(\bar{\alpha}\hat{u}_0-\beta)\hat{\varphi}'' - \varepsilon^{-3}\hat{v}_{0\hat{y}\hat{y}}\hat{\varphi}' - \varepsilon^{-1}\hat{v}_{0\hat{x}\hat{x}}\hat{\varphi}' - i\bar{\alpha}\hat{u}_{0\hat{y}\hat{y}}\hat{\varphi}] = 0. \tag{2.16}$$

For the transformation in Eq. (2.15), the $\hat{u}_0$-profile in Eq. (2.14) for $x_{sep}$ is more suitable since Eq. (2.13) applies only for $0 \leqslant \hat{y} \leqslant 1$.

The coefficient terms involving $\hat{v}_0$ in Eq. (2.16) can be determined from the uniformly valid $\hat{u}_0$-profile at $x_{sep}$ by making additional use of the triple-deck results. The $\hat{v}_0$-profile in a stretch corresponding to the main deck ($y = O(\varepsilon^4)$) can be obtained from the relation [12].

$$\hat{v}_0 = -\varepsilon^3\left(\frac{dA}{dx'}\right)\hat{u}_m(\hat{y}), \tag{2.17}$$

where $A(x')$ denotes the flow displacement due to the lower deck with $x' = \varepsilon^{-3}x$, $\hat{u}_m$ being the upstream boundary-layer profile (cf. Eq. (2.9)). $\hat{u}_m(\hat{y})$ may be in turn determined from the differential equation [12]

$$\hat{u}_m + \varepsilon A(x')\frac{d\hat{u}_m}{d\hat{y}} = \hat{u}_0, \tag{2.18}$$

where $\hat{u}_0$ stands for the corresponding portion of the given $\hat{u}_0$-profile in Eq. (2.14) or also Eq. (2.13). The values of $A(x')$ and its derivatives at $x_{sep}$ (for vanishing skin friction)

http://rcin.org.pl

are obtainable from the available results in [14]. The terms involving $\hat{v}_0$ in the region immediately adjacent to the wall and equivalent to the lower deck ($y = O(\varepsilon^5)$) are then approximated by linear correlation or polynomials. It is found that the shape of polynomials and the extent of the estimated depth of the wall region have little effect on the results of treating Eq. (2.16). The same is true for the stretch corresponding to the upper deck beyond $\hat{y} = 1$.

### 2.3. Analysis of instability

The stability analysis is carried out by use of Eq. (2.16) together with the boundary conditions by transforming Eq. (2.12) and with the velocity coefficients determined from Eq. (2.14) (and also Eq. (2.13)) as well as Eq. (2.17). Taking advantage of the linearity of (Eq. 2.16) and representing $\hat{\varphi}$ by a complex function such that $\hat{\varphi} = \hat{\varphi}_r + i\hat{\varphi}_i$, one obtains for the case of temporal instability with $\bar{\beta} = \beta_r + i\beta_i$ and with $f \equiv \hat{\varphi}$ ; $g \equiv \hat{\varphi}_i$ ($\bar{\alpha}$ real)

$$
\begin{aligned}
&f'''' - \varepsilon^{-3}\hat{v}_0 f''' - \bar{\beta}_i f'' + (\varepsilon^{-1}\hat{v}_{0\hat{x}\hat{x}} + \varepsilon^{-3}\hat{v}_{0\hat{y}\hat{y}})f' + (\bar{\alpha}\hat{u}_0 - \bar{\beta}_r)g'' - \bar{\alpha}\hat{u}_{0\hat{y}\hat{y}}g = 0,\\
&g'''' - \varepsilon^{-3}\hat{v}_0 g''' - \bar{\beta}_i g'' + (\varepsilon^{-1}\hat{v}_{0\hat{x}\hat{x}} + \varepsilon^{-3}\hat{v}_{0\hat{y}\hat{y}})g' - (\bar{\alpha}\hat{u}_0 - \bar{\beta}_r)f'' + \bar{\alpha}\hat{u}_{0\hat{y}\hat{y}}f = 0,
\end{aligned}
\tag{2.19}
$$

whereas for the case of spatial instability with $\bar{\alpha} = \bar{\alpha}_r + i\bar{\alpha}_i$ ($\bar{\beta}$ real)

$$
\begin{aligned}
&f'''' - \varepsilon^{-3}\hat{v}_0 f''' + \bar{\alpha}_i\hat{u}_0 f'' + (\varepsilon^{-1}\hat{v}_{0\hat{x}\hat{x}} + \varepsilon^{-3}\hat{v}_{0\hat{y}\hat{y}})f'\\
&\qquad - \bar{\alpha}_i\hat{u}_{0\hat{y}\hat{y}}f + (\bar{\alpha}_r\hat{u}_0 - \bar{\beta})g'' - \bar{\alpha}_r\hat{u}_{0\hat{y}\hat{y}}g = 0,\\
&g'''' - \varepsilon^{-3}\hat{v}_0 g''' + \bar{\alpha}_i\hat{u}_0 g'' + (\varepsilon^{-1}\hat{v}_{0\hat{x}\hat{x}} + \varepsilon^{-3}v_{0\hat{y}\hat{y}})g'\\
&\qquad - \bar{\alpha}_i\hat{u}_{0\hat{y}\hat{y}}g - (\bar{\alpha}_r\hat{u}_0 - \bar{\beta})f'' + \bar{\alpha}_r\hat{u}_{0\hat{y}\hat{y}}f = 0,
\end{aligned}
\tag{2.20}
$$

where $\hat{x}$ is identical with $x'(= \varepsilon^{-3}x)$.

In both cases, the analysis reduces to a simultaneous two-point eigenvalue problem for $f$ and $g$. The problems are treated by employing a shooting procedure incorporating a Runge–Kutta–Verner 5th and 6th-Order Method in combination with a Newton–Raphson iteration process for handling the boundary conditions. For both the temporal and spatial analyses, the boundary conditions are specified as $f' = 0, f'' = 0$; $g' = 0, g'' = 0$ at wall and at some appropriate tried-out outer boundary of the treated region.

In the present investigation both temporal and spatial instabilities have been studied. It is found that for the present case of separation instability the temporal stability analysis yields more and revealing information. This might be explicable by the fact that, in contrast to normal boundary-layer flows where velocity profiles are similar along the direction of flow, the velocity profiles generally change drastically along the main direction of flow in the separation region.

## 3. Results and discussion

Equations (2.11) and (2.16) deviate from the ordinary Orr–Sommerfeld equation in that terms with coefficients of the normal velocity component of the basic flow and its derivatives appear. This results from the assessment of the basic flow in the knowledge of the triple-deck analysis. By aid of Eq. (2.16), flows with $\mathrm{Re}_D$ up to 300 have been investigated in the present analysis. This roughly corresponds to the flow range prior to the

http://rcin.org.pl

beginning of noticeable fluctuating motion of the separation point(s) themselves. Because of the more revealing information attained by the analysis of temporal instability, results of such analysis are presented here.

For the various wave number $\bar{\alpha}$ and for the different frequencies $\bar{\beta}$ investigated, a limiting value of $\mathrm{Re}_D$ (critical Re) of about 60 can be determined, as shown in Figs. 3 and 4.

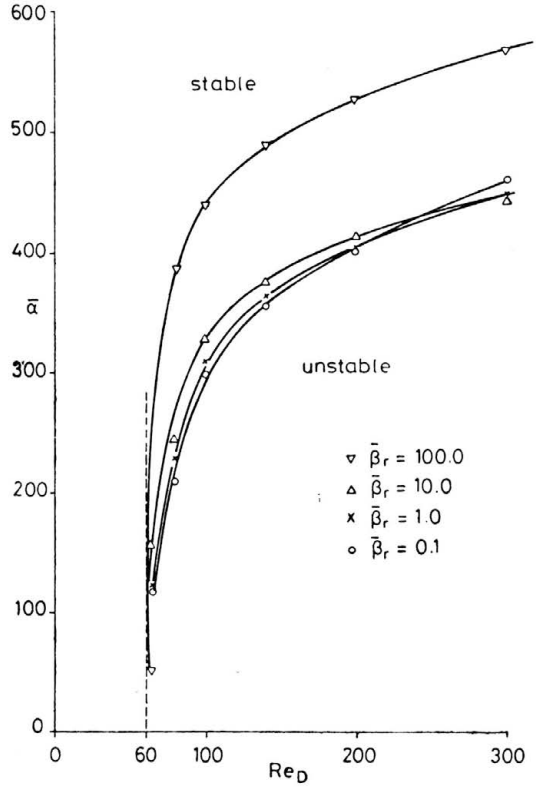


FIG. 3. Stability limits.

Figure 3 depicts the stability curve in the form of $\mathrm{Re}_D$ versus the wave number $\bar{\alpha}$, while Fig. 4 shows the stability curve with $\mathrm{Re}_D$ versus the frequency $\bar{\beta}_r$ or the real value of $\bar{\beta}$. According to the recent careful experimental investigation of the wake flow near a circular cylinder in [1], the critical $\mathrm{Re}_D$ in correspondence to the periodic vortex shedding is found to be about 48. In spite of the various simplifications and approximations made in the present analysis, the critical value of $\mathrm{Re}_D$ presently found is considered to be in good agreement with the experimental value measured in the near wake of a circular cylinder.

The more revealing feature of the results consists of the relationships found between $\bar{\alpha}$ and $\bar{\beta}_r$ at the maximum amplification of instability. In Figs. 5–7, the curves are shown along which distinct maximum $\bar{\beta}_i$ values occur forming notable contrast to the values of $\bar{\beta}_i$ in the neighbourhood. $\hat{u}_0$-profiles with different steepness (by taking different values of $n$ cf Eq. (2.14)) have been taken, yet the results are essentially similar. Above and below

http://rcin.org.pl

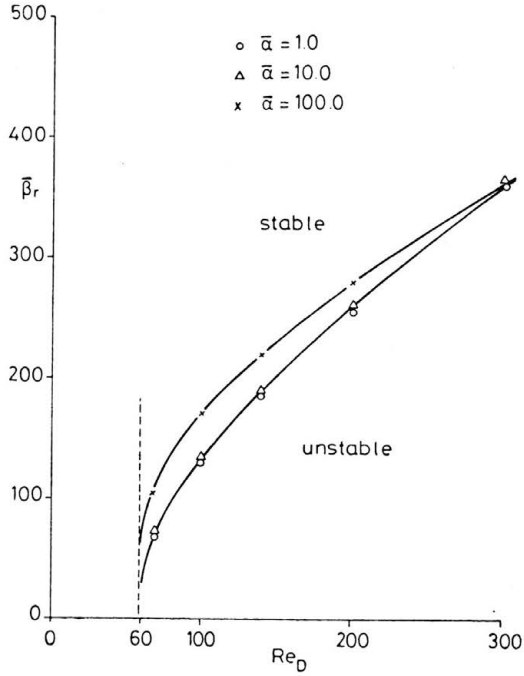


FIG. 4. Stability limits.

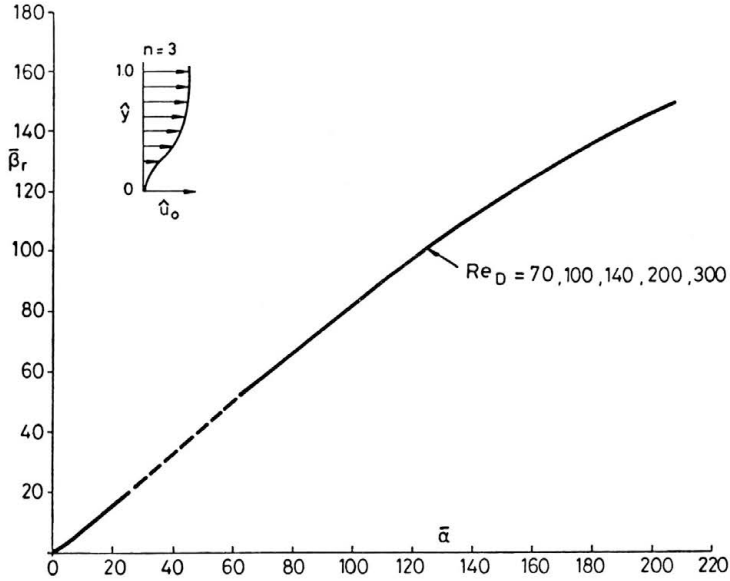


FIG. 5. Wave number-frequency relationship at maximum instability.

the curves in Figs. 5–7 the flows are largely unstable, while along the curves maximum growth rates of instability are reached. The maximum amplification relationships are relatively insensitive to $Re_D$. Broken stretches in the figures signify regions where the maximum amplification is not very pronounced. The most interesting range of the relationships

http://rcin.org.pl

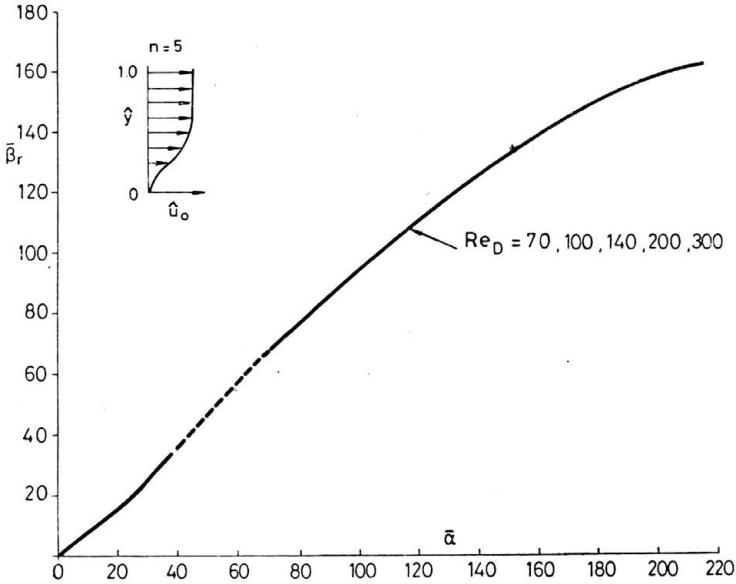


FIG. 6. Wave number-frequency relationship at maximum instability.

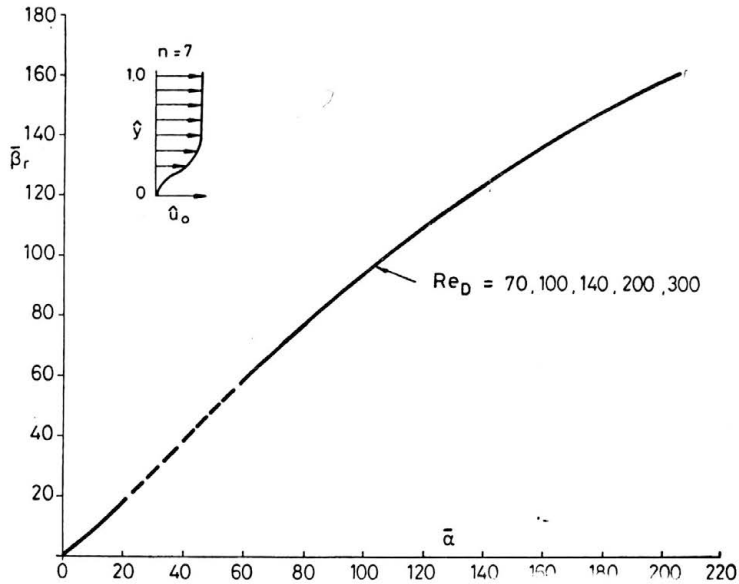


FIG. 7. Wave number-frequency relationship at maximum instability.

involves values of $\bar{\alpha}$ and $\bar{\beta}_r$ below 10. In this range the relationship between $\bar{\alpha}$ and $\bar{\beta}_r$ for maximum amplification is almost linear.

The notable aspect of the $\bar{\alpha}-\bar{\beta}_r$ relationship for maximum amplification from the present results consists in the apparent lack of preference for any definite combination

http://rcin.org.pl

of $\bar{\alpha}$ and $\bar{\beta}_r$ towards maximum amplification of instability. This implies that if some external signal in the form of, say, the resonance frequency of the wake instability is conveyed to the separation point, the most amplified wave disturbance will be of the wave length corresponding to the signal frequency in accordance with the $\bar{\alpha}-\bar{\beta}_r$ relationship for maximum amplification.

For a definite frequency $\bar{\beta}_r$, the $\bar{\alpha}-\bar{\beta}_r$ relationships for maximum amplification shown in Figs. 5–7 correspond in general to the lowest $\bar{\alpha}$ values (greatest wave lengths). For certain $\bar{\beta}_r$ values, comparably high amplifications at higher $\bar{\alpha}$ values forming near-multiples of the $\bar{\alpha}$ values given in the curves are noted. The appearance of these higher values with pronounced amplification is rather irregular and essentially limited to higher $\bar{\beta}_r$ values which lie beyond the range of practical interest. This means, however, that disturbances of fractional wave-lengths as compared to the values laid down by Figs. 5–7 might also be distinctly amplified, should there be any external excitation in the range of higher frequencies than are usually encountered. The implications of such aspects of instability are left for future investigations.

In line with the results obtained, a hypothesis may be advanced regarding the possible mechanism of the periodic vortex shedding. The periodic vortex shedding can arise from the maximum amplification of flow instability at the separation point triggered off by some external excitation, most probably by the resonance frequency of the near-wake instability as is explicable by the splitter-plate experiments. The near-wake investigations ([2]–[4]) have shown largely the pronounced instability of the wake flow against asymmetric disturbances. The asymmetric wake instability in turn can not only provide the triggering frequency for the separation instability but also evoke the alternating vortex shedding at both sides of the bluff body. To this extent, periodic vortex shedding might be regarded as the consequence of the combined action of wake instability and separation instability.

A rough estimate in alignment with the above hypothesis may be made for the case of flow about a circular cylinder. At $\mathrm{Re}_D = 100$, the Strouhal numbers (St) measured in the near wake by different investigators are: 0.167 [5]; 0.156 [16]; 0.150 [1]. These measured values for the near wake or some theoretically calculated near-wake values (e.g. [1] or [2]) may be taken as the triggering frequencies for the development of separation instability. Because of the relationships: $\bar{\beta}_r = 2\pi \cdot \mathrm{St}$ and $\lambda = \dfrac{2\pi D}{\bar{\alpha}}$ and the relationship at maximum amplification: $\bar{\alpha} \approx 1.5\bar{\beta}_r$ (e.g. for $n = 5$ in Fig. 6), the calculated values of $\bar{\beta}_r$ and thus of $\bar{\alpha}$ as well as $\lambda$ are tabulated below. If the ratio of the vortex spacing $l$ and the vortex-row spacing $h$ for the Kármán vortex street to be expected downstream is taken after Kármán as $l/h \approx 3.56$ and the calculated values of $\lambda$ are used for $l$, one obtains the tabulated $h/D$ values as below. These compare fairly well with the measured values of $h/D$ under comparable conditions in [5] which lie between 1.1 and 1.25.

| St | $\bar{\beta}_r$ | $\bar{\alpha}$ | $\lambda$ | $h/D$ |
|---|---|---|---|---|
| 0.167 | 1.049 | 1.574 | $3.992D$ | 1.121 |
| 0.156 | 0.980 | 1.470 | $4.274D$ | 1.200 |
| 0.150 | 0.942 | 1.417 | $4.434D$ | 1.245 |

http://rcin.org.pl

This estimate of course cannot serve as a logical check for the hypothesis set up previously, because, though the disturbance frequency is known to be relatively insensitive to nonlinearity, the amplitude and wave-length can be rather affected by nonlinear effects in the near wake region. Nevertheless, the rough estimate made above with the correct magnitude of the determined values does lend support to the conjecture about the mechanism of periodic vortex shedding.

## 4. Conclusions

The investigation of the two-dimensional laminar separation instability of an incompressible flow over a convex surface with a stability equation derived by the aid of results from the triple-deck asymptotic analysis shows that:

1. The separation instability yields a critical $\mathrm{Re}_D$ which lies at about 60 and corresponds well with the experimentally measured value in the near-wake region of a circular cylinder.

2. For the most interesting range of disturbances ($\bar{\alpha}$ and $\bar{\beta}_r$ below 10), a definite and almost linear relationship exists between the reduced wave number $\bar{\alpha}$ and frequency $\bar{\beta}_r$ for the maximum amplification of instability, yet the relationship reveals no specific preference for any definite combination of wave number and frequency.

3. Due to the apparent lack of any predestined combination of wave-length and frequency for the maximum amplification, it can be expected that some external agency such as the resonant frequency of the near-wake structural instability may act as a triggering device for the dominant amplification of some definite disturbance at the separation point. Moreover, the instability of the near-wake flow against asymmetric disturbances may conceivably contribute to the alternating vortex shedding at both sides of the bluff body.

4. The hypothesis seems to be justified that the periodic vortex shedding can be regarded as the result of a combined action of separation instability and near-wake structural instability. The estimated row spacings of the shedded vortices from a circular cylinder on the basis of the hypothesis tally well with the measured values.

## Acknowledgement

The author wishes to acknowledge with gratitude the kind help of Professor ZHU ZICHIANG of the Beijing (Peking) Institute of Aeronautics and Astronautics during his stay at DFVLR in modelling the numerical treatment of the subject problem. Thanks are also due to Dr. G. R. SARMA and Dr. U. DALLMANN for their helpful discussions relating to the subject.

## References

1. M. NISHIOKA, H. SATO, *Mechnism of determination of the shedding frequency of vortices behind a cylinder at low Reynolds numbers*, J. Fl. Mech., **89**, Pt. 1, 49–60, 1978.
2. R. BETCHOV, W. O. CRIMINALE, *Spatial instability of the invisicd jet and wake*, Phys. of Fl., **9**, 359–362, 1960.



http://rcin.org.pl

3. H. OERTEL, *Vortices in wakes induced by shock waves*, Proc. 14th Symposium on Shock Tubes and Waves, Sydney, Australia, 1983.
4. W. KOCH, *Organized structures in wakes and jets — an aerodynamic resonance phenomenon?*, Proc. 4th Symposium on Turbulent Shear Flows, Karlsruhe, Germany, 1983.
5. A. ROSHKO, *On the drag and shedding frequency of two-dimensional bluff bodies*, NACA TN 3169, 1954.
6. A. ROSHKO, *On the wake and drag of bluff bodies*, J. Aero. Sci., **22**, 124–132, 1955.
7. A. ROSHKO, *Experiments on the flow past a circular cylinder at very high Reynolds number*, J. Fl. Mech., **10**, 345–356, 1961.
8. J. PRETSCH, *Die Stabilität einer ebenen Laminarströmung bei Druckgefälle und Druckanstieg*, Jahrbuch der deutschen Luftfahrtforschung, 58–75, 1941.
9. T. H. HUGHES, W. H. REID, *The stability of laminar boundary layers at separation*, J. Fl. Mech., **23**, 737–747, 1965.
10. A. R. WAZZAN, T. T. OKAMURA, A. M. O. SMITH, *Stability of laminar boundary layers at separation*, Phys. of Fl., **10**, 2540–2545, 1967.
11. S. GOLDSTEIN (Editor), *Modern developments in fluid dynamics*, Oxford University Press 1938.
12. K. STEWARTSON, *Multistructured boundary layers on flat plates and related bodies*, Adv. Appl. Mech., **14**, 145–239, 1974.
13. V. V. SYCHEV, *Concerning laminar separation*, Izv. Akad. Nauk SSSR Mekh, Zhidk Gaza, **3**, 47–59, 1972.
14. F. T. SMITH, *The laminar separation of an incompressible fluid streaming past a smooth surface*, Proc. Royal Soc. London A 356, 443–463, 1977.
15. A. F. MESSITER, R. L. ENLOW, *A model for laminar boundary-layer flow near a separation point*, SIAM J. Appl. Math., **25**, 655–670, 1973.
16. E. BERGER, R. WILLE, *Periodic flow phenomena*, Ann. Rev. Fl. Mech., **4**, 313–340, 1972.

**DFVLR-INSTITUTE FOR THEORETICAL FLUID MECHANICS.**
**GÖTTINGEN, FRG.**

*Received October* 28, 1983.

http://rcin.org.pl